

AEROSOL FORMATION FROM THE REACTION OF α -PINENE AND OZONE USING A GAS PHASE KINETICS-PARTICLE PARTITIONING MODEL

R.M. Kamens, M. Jaoui, S. Lee, C.J.Chien
Department of Environmental Sciences and Engineering,
University of North Carolina, Chapel Hill, NC 27599-7400, USA
e-mail: kamens@unc.edu
fax: 919 966-7911

11-17-99, Bangkok, Thailand

ABSTRACT

A kinetic mechanism was used to describe the gas-phase reactions of α -pinene with ozone. This reaction scheme produces low vapor pressure reaction products that distribute between gas and particle phases. Partitioning was treated as an equilibrium between the rate of particle uptake and rate of particle loss of semivolatile terpene reaction products. Given estimated liquid vapor pressures and activation energies of desorption, it was possible to calculate gas-particle equilibrium constants and aerosol desorption rate constants at different temperatures. Gas and aerosol phase reactions were linked together in one chemical mechanism and a chemical kinetics solver was used to predict reactant and product concentrations over time. Aerosol formation from the model was then compared with aerosol production observed from outdoor chamber experiments. Approximately 10-40% of the reacted α -pinene carbon appeared in the aerosol phase. Models vs. experimental aerosol yields illustrate that reasonable predictions of secondary aerosol formation are possible from both dark ozone and light/NO_x α -pinene systems.

INTRODUCTION

The atmospheric chemistry of non-methane biogenic hydrocarbons has received much attention because of their significant global emissions, high photochemical reactivity, and their high aerosol forming potential. Although the potential of aerosol formation from terpenes was noted as early as 1960 by Went¹, the magnitude of the natural contribution by biogenics to the particulate burden in the atmosphere is still not well characterized. In this paper, we will describe the feasibility of a predictive technique for the formation of secondary aerosols from biogenic hydrocarbons. An advantage of this approach is that it has the ability to embrace the range of different atmospheric chemical and physical conditions that bring about secondary aerosol formation.

EXPERIMENTAL SECTION

Gas-particle samples for this study were generated in a large outdoor 190 m³ Teflon film chamber (Kamens et al., 1995, Fan et al., 1996). All experiments were carried out under darkness to exclude photochemical effects. Rural background air was used to charge the chamber without not any additional injections of oxides of nitrogen. Secondary aerosols were created by the

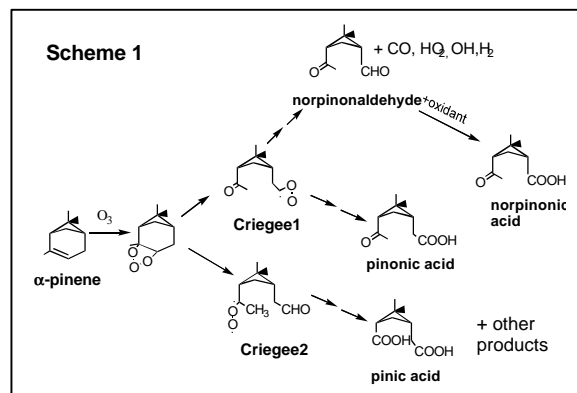
reaction of α -pinene with O_3 in the chamber. O_3 from an electric discharge ozone generator was added to the chamber over the course of an hour with initial concentrations ranging, depending on the experiment, from 0.25 to 0.65 ppm. It was measured using a Bendex chemiluminescent O_3 meter (model 8002, Roncerverte, WV) and calibrated via gas phase titration using a NIST traceable NO tank. O_3 addition to the chamber was followed by volatilizing, depending on the experiment, 0.4 to 1 mL of liquid α -pinene into the chamber atmosphere. The gas-phase concentration of α -pinene was monitored with an online gas chromatograph (Shimadzu Model 8A, column: 1.5 m, 3.2 mm stainless steel packed with Supelco 5% Bentanone 34) using a flame ionization detector, and calibrated with a known concentration of a mixture of toluene and propylene.

Gas and particle phase α -pinene products were simultaneously collected with a sampling train that consisted of an upstream 5-channel annular denuder, followed by a 47mm Teflon glass fiber filter (type T60A20, Pallflex Products Corp., Putnam, CT, USA) and another denuder. In one of the experiments, a parallel sampling system consisting of a filter, followed by a denuder was also used. The details of the sample workup procedure and quantitative analysis have been reported in previous manuscripts Kamens et al., 1995 and Fan et al., 1996). Carbonyl products of α -pinene- O_3 aerosols were derivatized by O-(2,3,4,5,6-pentafluorobenzyl)hydroxyl-amine hydrochloride (PFBHA) as described by Yu et al., 1997, and carboxylic acids, using pentafluorobenzyl bromide (PFBBR) as a derivatizing agent as described by Chien et al., (1998). (\pm)- α -Pinene, O-(2,3,4,5,6-pentafluorobenzyl)hydroxylamine hydrochloride (PFBHA), pentafluorobenzylbromide (PFBBR), decafluorobibenzyl (internal standard for derivatization), cis-pinonic acid, n-hexanoic acid, n-octanoic acid, hexane-1,6-dionic acid, and heptane-1,7-dionic acid were all purchased from Aldrich (Milwaukee, WI).

In one of the experiments the particle size distribution and aerosol concentration for particles ranging from 0.018 to 1.0 μ m were monitored by an Electrical Aerosol Analyzer (EAA) (Thermo Systems, Inc., Model 3030, Minneapolis, MN). Total aerosol number concentration was also measured by a Condensation Nuclei Counter (CNC, Model Rich 100, Environment One Corp., Schenectady, NY).

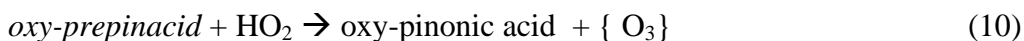
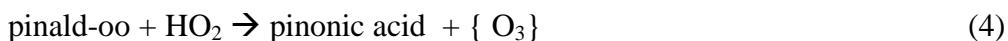
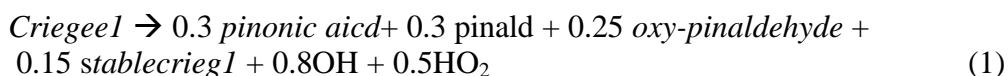
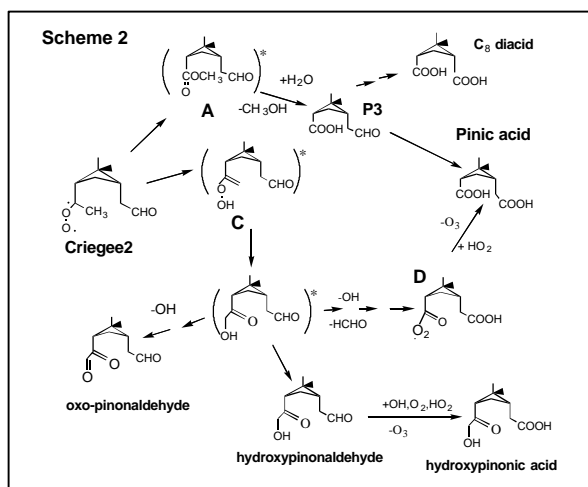
A GAS-PARTICLE MECHANISM

As a result of new aerosol compositional information (Jang and Kamens, 1999, Yu et al., 1998) we have developed an exploratory model for predicting aerosol yields from the reaction of α -pinene with ozone in the atmosphere. Reaction pathways (Scheme 1 and 2) were constructed from experimentally measured products which include: pinonaldehyde, norpinonaldehyde, pinonic acid, norpinonic acid, pinic acid, 2,2-dimethylcyclobutane-1,3-dicarboxylic acid, and hydroxy and aldehyde substituted pinonaldehydes and hydroxy pinonic acids. To simplify the mechanism in this study, six generalized semivolatile products were defined: 1. “*pinald*” to represent pinonaldehyde and norpinonaldehyde, 2. “*pinacid*” to represent pinonic and norpinonic acids, 3. “*diacid*” for pinic acid and norpinic acid, (2,2-dimethylcyclobutane-1,3-dicarboxylic acid), 4. “*oxy-pinald*” for hydroxy and aldehyde substituted pinonaldehydes (called oxo-substituted), 5. “*P3*” for 2,2-dimethylcyclobutyl-3-acetylcarboxylic acid, (a pinic acid precursor), and 6. “*oxy-pinacid*” for hydroxy and aldehyde substituted pinonic acids. A last group, *frag*, was employed to account for volatile oxygenated products.



“*pinald*” to represent pinonaldehyde and norpinonaldehyde, 2. “*pinacid*” to represent pinonic and norpinonic acids, 3. “*diacid*” for pinic acid and norpinic acid, (2,2-dimethylcyclobutane-1,3-dicarboxylic acid), 4. “*oxy-pinald*” for hydroxy and aldehyde substituted pinonaldehydes (called oxo-substituted), 5. “*P3*” for 2,2-dimethylcyclobutyl-3-acetylcarboxylic acid, (a pinic acid precursor), and 6. “*oxy-pinacid*” for hydroxy and aldehyde substituted pinonic acids. A last group, *frag*, was employed to account for volatile oxygenated products.

A kinetic mechanism was used to describe the gas-phase reactions of α -pinene with ozone. One of the products, pinic acid, a dicarboxylic acid, has a subcooled liquid vapor pressure of $\sim 10^{-6}$ mmHg at 295K, which may be low enough to initiate self nucleation. More volatile products such as pinonic acid and pinonaldehyde, will not self-nucleate, but will partition onto existing particles. Gas and aerosol phase reactions are linked together in one chemical mechanism and a chemical kinetics solver (Jeffries, 1991) is used to predict reactant and product concentrations over time. Gas phase rate constants are available for a number of these reactions (Atkinson, 1997). These reactions were then added to the inorganic chemistry reactions of the Carbon Bond 4 photochemical mechanism [Gery et al., 1989]. Reactions of Criegee 1 and 2 biradicals in Scheme 1 & 2, and OH attack on α -pinene are partially described below as:



Partitioning is treated as an equilibrium between the rate of particle up-take and the rate of particle loss of individual semivolatile α -pinene reaction products. The ratio of the rate constants for the forward and backward reactions k_{on}/k_{off} is equal to the equilibrium constant, K_p , for the

gas-particle equilibrium of a given partitioning compound i .

$${}^iK_p = {}^i k_{\text{on}} / {}^i k_{\text{off}} \quad (11)$$

It is assumed that secondary aerosols are liquid-like, and iK_p can be calculated from gas-liquid (absorptive) partitioning theory, as described by Pankow (1994).

$$\log {}^iK_p = -\log {}^iP_L^o - \log {}^i\gamma_{\text{om}} + \text{constant} \quad (12)$$

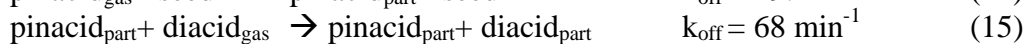
From estimated vapor pressures, ${}^iP_L^o$ (Kamens et al., 1999) and calculated activity coefficients, ${}^i\gamma_{\text{om}}$, which are close to one in these aerosols (Jang et al., 1997) iK_p can be calculated for the reaction products. The rate constant, k_{off} , for loss of a compound from the liquid particle phase to the gas phase has the form $k_{\text{off}} = \beta e^{-E_a/R}$. β can be evaluated and the activation energy, E_a estimated (Kamens et al., 1999). This then permits an estimate of the rate of absorption ${}^i k_{\text{on}}$ from the gas phase.

In the model *seed* nuclei provide initial liquid volumes for gas-liquid partitioning. The product compounds that actually participate in the self nucleation process are as yet unknown. One possibility is that the stabilized Criegee radical (*stabcrieg1* and *stabcrieg2*) reacts with the carbonyl portion of product compounds to produce an extremely low pressure secondary ozonide product. These types of products have been observed from an O₃- propylene system by Niki and co-workers (1997) and more recently by Neeb et al., 1995) for larger molecules]. It is also possible to form an anhydride from the reaction of the Criegee with a dicarboxylic acid (Neeb et al., 1996). In the α -pinene case, these products would have molecular weights of ~ 350 , and be of extremely low volatility. By techniques described previously (Kamens et al., 1999) vapor pressures lower than 10^{-15} torr are estimated, and \sim one second after the start of the experiments in this study, would exceed supersaturation by ~ 1000 fold. This suggests these compounds would most certainly self nucleate. In our mechanism these are called “*seed1*” particles. We assumed that stabilized Criegees would react with all carbonyl products. For example:



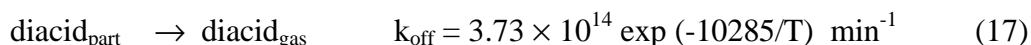
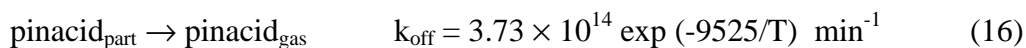
This process was not very important for the experiments in this study, given the background nucleation levels that resulted during the injection of α -pinene into the chamber. Predictions, using the model developed here, however, suggest a strong influence of these seeds on particle formation when α -pinene has concentrations of ~ 5 ppb. Gas phase products migrate to the particle phase and then create more mass for additional partitioning.

Once seed surfaces are available, the migration of gas phase products such as pinonic acid ($\text{pinacid}_{\text{gas}}$) on to *seed1* particles to give pinacid particle phase ($\text{pinacid}_{\text{part}}$) and diacid gas product on to the newly formed $\text{pinacid}_{\text{part}}$ to form pinic diacid particle phase ($\text{diacid}_{\text{part}}$) can thus be represented as:



To conserve mass, the amount of $\text{diacid}_{\text{part}}$ and $\text{pinacid}_{\text{part}}$ mass appears on both sides of the equation. To maintain equilibrium, both $\text{diacid}_{\text{part}}$ and $\text{pinacid}_{\text{part}}$ back reacts or “off-gases” from the particle to give back gas phase pinonic acid. A similar set of reactions can be written for all of

the partitioning products.

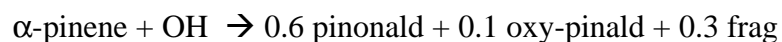


MODEL AND CHAMBER DATA COMPARISONS

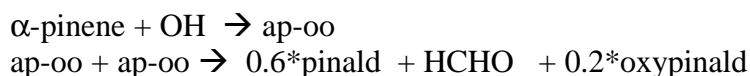
Aerosol formation from the model is compared with aerosol production determined from 190 m³ dark outdoor chamber experiments. The actual rate constants and mechanism used are summarized in Table 1. The main updates since our first publication of the mechanism (Kamens et al, 1999) are:

1. An increase in the rate constant for the OH attack on pinonaldehyde from $2.4 \times 10^{-12} \text{ cm}^3 \text{ molecule}^{-1} \text{ sec}^{-1}$ (as per to Kwok and Atkinson, 1995) to their more recent value of $\sim 5 \times 10^{-12} \text{ cm}^3 \text{ molecule}^{-1} \text{ sec}^{-1}$.

2. We replaced the reaction



with



This was done to more easily add NO oxidation reactions by the hydroxy-peroxy-radical, ap-oo. In addition, the previously used lumped reaction may over estimate the pinonaldehyde yield from OH attack on α -pinene in the absence of NOx.

3. We lowered the k_{on} values for all absorbing species because it is more appropriated to use the the average molecular weight of the aerosol in converting from Kp units of

Given the offsetting nature of the above changes, model simulations vs. experimental data for α -pinene, O₃ and aerosol yields for a warm (295K) and a cool outdoor experiment (285K) showed little difference (Figure 1) between our originally published simulations and the updated mechanism (Kamens et al, 1999.) Approximately 20-40% of the reacted α -pinene carbon appears in the aerosol phase. Under cool conditions (285K), both measurements and model predictions suggest that pinonaldehyde is the major gas phase product, while pinic acid, pinonic acid, hydroxy-pinonaldehydes, and hydroxy-pinonic acids are the major aerosol phase products. Under warm conditions, the predicted major gas phase product are pinonaldehyde, hydroxy-pinonaldehydes, some pinonic acid, and a trace of dicarboxylic acid. The particle phase was dominated by pinic acid followed by pinonic acids, hydroxy-pinonaldehydes, and hydroxypinonic acids. The important observation is that the aerosol composition seems to differ radically between warm and cool experiments and this is consistent with the observations of Jang and Kamens (1999).

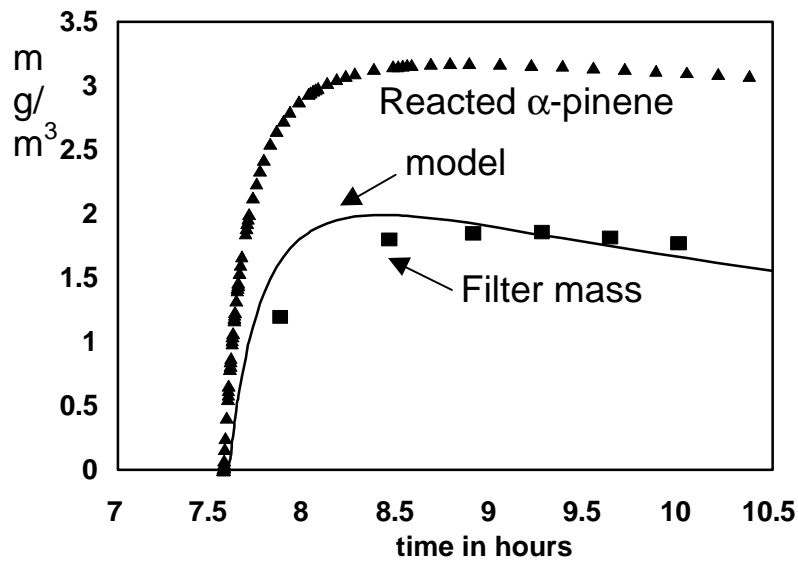
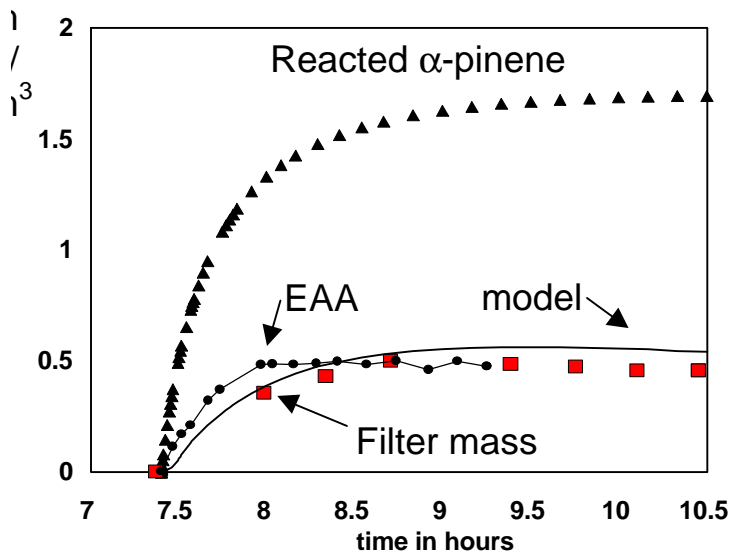
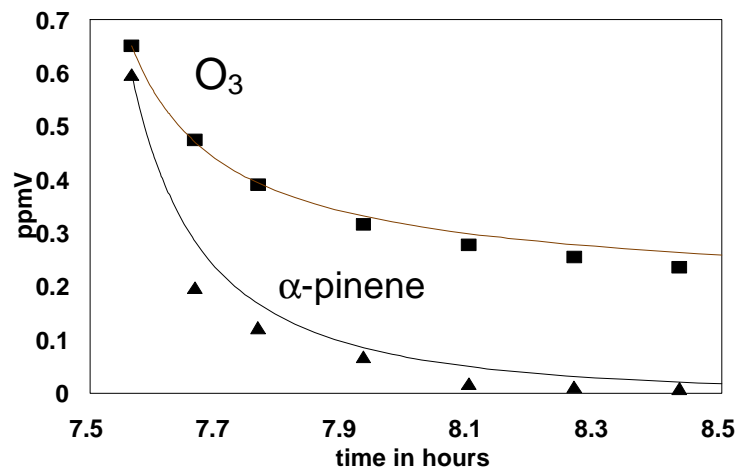
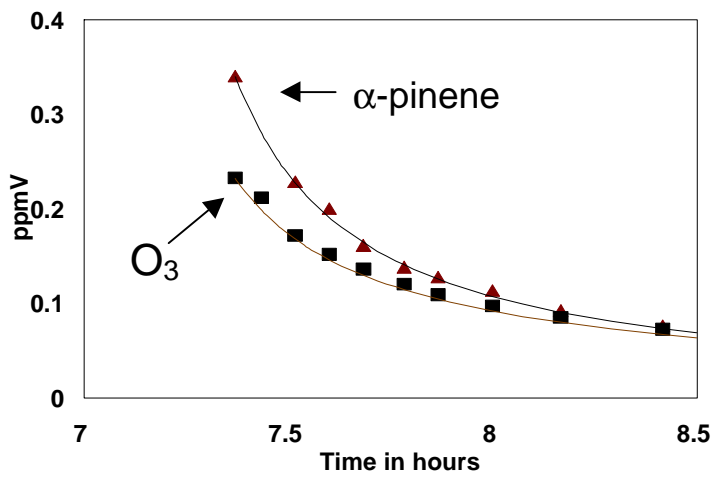


Figure 1. Model and experimental data from a warm (top and bottom left panels) and cool (top and bottom right panels) outdoor chamber experiment performed under darkness with α

3

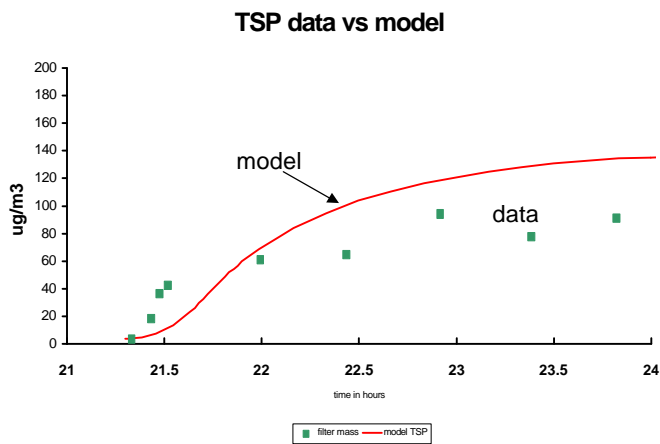


Figure 3. Particle data and model for the dark reaction of 0.20 ppmV α -pinene with 0.12 ppm O_3 at 297K.

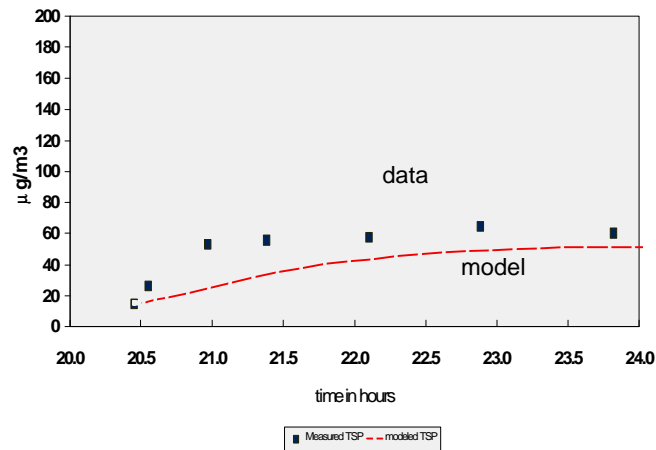


Figure 4. Particle data and model for the dark reaction of 0.12 ppmV α -pinene with 0.06 ppm O_3 at 299K.

During the summer of 1999 two relatively low concentration experiments were conducted and as shown in Figures 3 and 4 these data are fit reasonably well the model in its current form.

Given the above mechanism, it was not difficult to implement a day time model that would involve the oxidation of NO to NO₂ and the formation of PAH analogue compounds. What is unknown is the quantum yields for propinaldehyde type compounds, so as a default, the quantum yields and cross sections for methylglyoxal were used. Hydroxy-nitrated α -pinene products (OH-apNO₃) and PAN analog compounds were partitioned to the particle phase as per the methodology described above. Although these reactions are not completely described in by the dark mechanism in Table 1, our fit to a daytime experiment with 0.97 ppm of α -pinene and 0.44 ppm NO_x is shown in Figure 5. It is clear that the current mechanism does not characterize all of the processes involved in the oxidation of NO_x and we also over predict the amount of ozone that is formed. What is encouraging is that we show the same trend in the ozone behavior as the data, and the model gives a reasonable fit to the filter based particle data (Figure 6). We also show reasonable fits to product pinonaldehyde in both the gas and the particle phases. Product model data also suggest that nitrated compounds can dominate the particle phase.

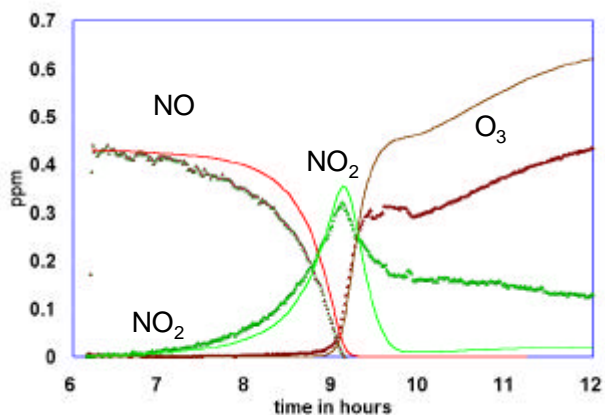


Figure 5. NO_x and O₃ data and model fit for the daytime reaction of 0.097 ppmV α -pinene with 0.44 ppm NO_x on June 9, 1999. Lines are the model and heavy lines-symbols are the data

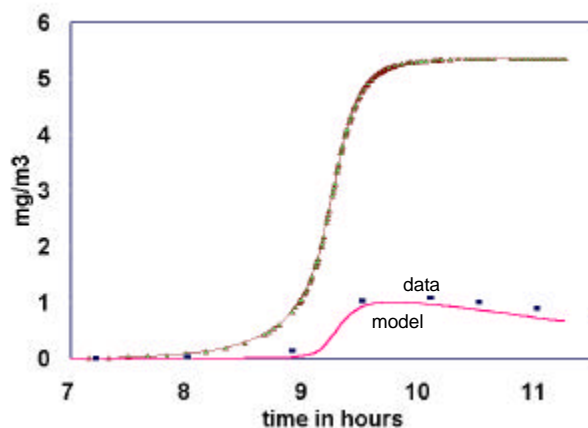


Figure 6. Particle data and model for the daytime reaction of 0.097 ppmV α -pinene with 0.44 ppm NO_x on June 9, 1999.

Table 1. Gas and particle phase reactions used to simulate secondary aerosol formation.

gas phase reactions

min⁻¹ or ppm⁻¹ min⁻¹

1. α -pinene + O₃ → .4 Criegee1 + .6 Criegee2 1.492 exp-732/T,
2. Criegee1 → .3 pinacid_{gas} + .15 stabcrieg1 + .8 OH + .5 HO₂ 1x10⁶,
 + .3 pinald_{gas} + .25 oxy-pinald_{gas} + .3 CO
3. Criegee2 → .3 crgprod2 + .55oxy-pinald_{gas} + .35 HCHO 1000,
 + .15 stabcrieg2 + .8 OH + .5 HO₂

4. stabcrieg1 + H ₂ O	→ pinacid _{gas}	1x10 ⁶ ,
5. stabcrieg2 + H ₂ O	→ P3 _{gas} (pinalic acid) + CH ₃ OH	6x10 ⁻³ ,
6. P3 _{gas} + OH	→ predi-oo	72380,
7. oxy-pinald + OH	→ oxy-prepinacid	72380,
8. predi-oo + HO ₂	→ diacid _{gas}	677 exp1040/T,
9. crgprod2 + HO ₂	→ diacid _{gas}	677 exp1040/T,
10. oxy-prepinacid + HO ₂	→ oxy-pinacid	677 exp1040/T
11. OH + apine	→ ap-oo	17873 @444,
12. ap-oo + NO	→ 0.85*NO ₂ + 0.67*pinald + 0.13*oxypinald + 0.65*HO ₂ + 0.17*HCHO + 0.15*OH-apNO ₃ + 0.07*acetone	5482.1 @ 242,
13. ap-oo + ap-oo	→ 0.6*pinald + HCHO + 0.2*oxypinald	4000,
14. α-pinene + NO ₃	→ 0.7*pinald + 0.2*OH-apNO ₃ {+ 0.05*oxydiNO ₃ }	544 @818,
15. pinald + OH	→ pinald-oo	72380,
15. pinald-oo + HO ₂	→ pinacid _{gas}	677 exp1040/T,
17. diacid _{gas} {walls}	→	6x10 ⁻⁷ exp2445/T,
18. oxy-pinacid _{gas} {walls}	→	6x10 ⁻⁷ exp2445/T,
19. pinacid _{gas} {walls}	→	4x10 ⁻⁷ exp2445/T,
20. oxy-pinald _{gas} {walls}	→	4x10 ⁻⁷ exp2445/T,
21. pinald _{gas} {walls}	→	2.5x10 ⁻⁷ exp2445/T,

partitioning reactions

22. stabcrieg1 + pinald _{gas}	→ seed1	29.5,
23. stabcrieg2 + oxy-pinald _{gas}	→ seed1	29.5
24. stabcrieg2 + HCHO	→ oxy-pinald	29.5,
25. pinacid _{gas} + seed1	→ seed1 + pinacid _{part}	19.4,
26. pinacid _{gas} + diacid _{part}	→ diacid _{part} + pinacid _{part}	19.4,
27. pinacid _{gas} + seed	→ seed + pinacid _{part}	19.4,
28. pinacid _{gas} + pinacid _{part}	→ pinacid _{part} + pinacid _{part}	19.4,
29. pinacid _{gas} + pinacid _{part}	→ pinacid _{part} + pinacid _{part}	19.4,
30. pinacid _{gas} + oxy-pinald _{part}	→ oxy-pinald _{part} + pinacid _{part}	19.4,
31. pinacid _{gas} + P3 _{part}	→ P3 _{part} + pinacid _{part}	19.4,
32. pinacid _{gas} + oxy-pinacid _{part}	→ oxy-pinacid _{part} + pinacid _{part}	19.4,
33. pinacid _{part}	→ pinacid _{gas}	3.73x10 ¹⁴ exp-9525/T
34. diacid _{gas} + pinacid _{part}	--> pinacid _{part} + diacid _{part}	68
35. diacid _{part}	→ diacid _{gas}	3.73x10 ¹⁴ exp-10285/T,
36. pinald _{gas} + oxy-pinacid _{part}	→ oxy-pinacid _{part} + pinald _{part}	4.2,
37. pinald _{part}	→ pinald _{gas}	3.73x10 ¹⁴ exp-8598/T,
38. oxy-pinald _{gas} + P3 _{part}	→ P3 _{part} + oxy-pinald _{part}	14.1,
39. oxy-pinald _{part}	→ oxy-pinald _{gas}	3.73x10 ¹⁴ exp-9341/T,
40. p3 _{gas} + oxy-pinacid _{part}	→ oxy-pinacid _{part} + p3 _{part}	13,
41. p3 _{part}	→ p3 _{gas}	3.73x10 ¹⁴ exp-9282/T,
42. oxy-pinacid _{gas} + seed1	→ seed1 + oxy-pinacid _{part}	74,
43. oxy-pinald _{part}	→ oxy-pinacid _{gas}	3.73x10 ¹⁴ exp-10353/T
44. diacid _{part} {walls}	→	0.0008,
45. O ₃ {walls}	→	0.0005,

*Rate constants are at 298K. To convert the 2nd order rate constant in cm³ molecule⁻¹ sec⁻¹ in the text to ppm⁻¹ min⁻¹, divide the rate constant in cm³ molecule⁻¹ sec⁻¹ by 6.77x10⁻¹⁶. **exp in the temperature dependent reactions is the natural base e, in the rate equation, k = B e^{-A/T}. The gas constant R is imbedded in A so that A = E_a/R. ***The partitioning reactions for *pinald*, *oxy-pinald*, *diacid*, and *oxy-pinacid*, are the same as for the *pinacid*, but to save space, are only given for k_{off} and one particle species. *stabcrieg1* and *stabcrieg2* reactions are illustrated for *pinacid_{gas}*, and *oxy-*

*pinacid*_{gas} and HCHO, but are the same for the other carbonyls. Loss of product gases to the chamber walls were estimated from observed pyrene loss at 297 and 271K. References for reactions are give in Kamens et al., (1999) were determined in this study. All reactants were diluted from the chamber at a rate determined with an SF₆ tracer. A typical loss was 0.0005 min⁻¹, Other specific measured or estimated losses like O₃, particles and α-pinene product to the walls, were adjusted for the SF₆ loss rate.

REFERENCES

- Atkinson, R. *J. Phys. Chem. Ref. Data*, **1997**, 26, 215-290
- Kwok, E.; Atkinson, R. *Atmos. Environ.*, **1995**, 29, 1685-1695.
- Chien, C. J.; Charles, M. J.; Sexton, K. G.; Jeffries, H. E. *Environ. Sci. Technol.* **1998**, 32, 299-309.
- Fan, Z.; Kamens, R. M.; Hu, J.; Zhang, J. *Environ. Sci. Technol.* **1996**, 30, 1359-1364.
- Grosjean, D.; Williams II, E. L.; Grosjean, E. *Environ. Sci. Technol.* **1993**, 27, 830-840.
- Jang, M.; Kamens R. M. *Atmos. Environ.* **1999**, 33, 459-474
- Jeffries, H. E. "PC-Photochemical Kinetics Simulation System (PC-PKSS), Software Version 3.0", **1991**, Department of Environmental Sciences and Engineering, School of Public Health, University of North Carolina, Chapel Hill, NC 27599.
- Gery, M. W.; Whitten, G. Z.; Killus, J. P.; Dodge, M. C. *J. Geophys. Res.* **1989**, 94, 12925-12956.
- Jang, M.; Kamens, R. M.; Leach, K.; Strommen, M. R. *Environ. Sci. Technol.* **1997**, 31, 2805-2811.
- Kamens, R. M.; Odum, J.; Fan, Z. *Environ. Sci. Technol.* 1995, 29, 43-50.
- Kamens, R. M.; Jang, M.; Leach, B. K.; Chien, C. "An Exploratory Kinetics and Gas-Particle Partitioning Model for Aerosol Formation From α -pinene- O_3 systems", *Environ Sci and Technol.*, in press May, 1999.
- Lyman, W. J.; Reehl, W. F.; Rosenblatt, D.H; Handbook of Chemical Property Estimation Methods, Environmental Behavior of Organic Compounds, American Chemical Society, Wash. D.C., 1990
- Moortgat, G.K.; Veyret, B.; Lesclaux, R. *Chem. Phys. Lett.*, **1989**, 160, 443-447.
- Niki, H.; Maker, P. D.; Savage, C. M., Breitenbach, L. P. *Chem. Phys. Lett.*, **1977**, 46, 327-330.
- Neeb, P.; Horie, O.; Moortgat, G. K. *Tetrahedron Lett.*, **1996**, 37, 9297-9300.
- Neeb, P.; Horie, O.; Moortgat, G.K. *Chem. Phys Lett.*, **1995**, 150-156
- Pankow, J. F. *Atmos. Environ.* **1994**, 28, 185-188.
- Yu, J.; Jeffries, H. E.; Le Lacheur, R. M. *Environ. Sci. Technol.* **1995**, 100, 1923-1932.
- Went, F. W., *Nature* **1960**, 187, 641-643.
- Yu, J.; Flagan, R.C.; Seinfeld J.H. *Environ. Sci. Technol.* **1998**, 32, 2357-2370.